





Effect of Fibers Orientation on the Nonlinear Dynamic Performance of Laminated Composite Plate under Different Loading In-plane

Wisam Hamzah Mohammed^{1,2*}, Svetlana Shambina¹ , Haider Kadhim Ammash² 

¹ Peoples Friendship University of Russia (RUDN University); 6 Miklukho-Maklaya Street, Moscow, 117198, Russian Federation.

² Department of Civil Engineering, University of Al-Qadisiyah, Al Diwaniyah, Iraq.

Received 21 August 2022; Revised 29 October 2022; Accepted 09 November 2022; Published 01 December 2022

Abstract

Non-linear dynamic analysis of a cross-ply laminated composite with fibre spacing plates under in-plane loading was presented. The mathematical formulation is based on first-order shear deformation theory and von-Karman non-linearity. Eight-node isoperimetric quadrilateral elements with five degrees of freedom per node were used to maintain geometric nonlinearity. In this investigation, a variety of fiber spacings and fibre orientations were used for the purpose of studying the effect of improvements on the behaviour of samples with this type of load. The dynamic equilibrium equations were solved using the Newmark integration technique. The non-linear dynamic analysis addressed several functions of changing fibre spacing with various changes in volume percentage and diverse fibre orientations. Fibre orientation, volume fraction fluctuation, and fibre distribution significantly affected laminated composite plates' non-linear dynamic behaviour. This study showed that the combination of improvements does not give a clear vision of the ideal improvement, and the best case for fibre distribution and the best case for layer rotation and combination should be studied to know the effect of the ameliorations one on the other and distinguish the impact of the transverse loading pattern in one direction on rotating the sample layers with axial load in one direction, so that changing the fibre distribution is more effective in the behaviour and stability of the plate by taking advantage of the orientation change, as demonstrated in this paper.

Keywords: Composite Laminated Plates; Orientation Fibres; Dynamic Stability; Elastic-Plastic Displacement; Response; Oscillations.

1. Introduction

In the early 1990s, the concept of spatially directing fibre pathways in the plane of a composite laminate was introduced [1]. Composite plates have been widely employed in many engineering applications such as structural, marine, and aerospace applications because of their superior mechanical properties [2], such as a light weight and high strength/stiffness-to-weight ratio. The high dynamic forces that are subjected on the structures constructed by this type of panels, which are often air impacts and have frequencies close to the ranges frequencies of these structures, which leads to exceeding the permissible levels of vibration [3], this makes the study of non-linear dynamic behaviour and composite laminated plate resistance to deformation when exposed to varied loads and boundary conditions vital for the safety of structures constructed of these plates and access to the most accurate risk evaluation of these structures to, for this the studies branched out to include the effect of loadings characteristics (boundary conditions, type ,magnitude ,direction, time period) [4], geometrical parameters (aspect ratio, slenderness ratio, shape and thickness regularity or thickness ratio) [5 , 6], mass matrix characteristics (general materials properties, orientation fiber and pattern distribution fiber) damping ratio and stiffener [7]. The procedure for calculating and designing structures made of composite materials is rather complicated; it requires the consideration of their real properties. Therefore, the problems of strain, dynamic stability, and oscillations in thin-walled structures made of composite materials are of great interest.

* Corresponding author: <mailto:1042198083@pfur.ru>



<http://dx.doi.org/10.28991/CEJ-2022-08-12-03>



© 2022 by the authors. Licensee C.E.J, Tehran, Iran. This article is an open access article distributed under the terms and conditions of the Creative Commons Attribution (CC-BY) license (<http://creativecommons.org/licenses/by/4.0/>).

Thin-walled structures such as plates, panels and shells often play the role of a bearing surface, to which certain elements of the structure are fixed. Such elements are pads [8], wherefore, the researchers studied the effects and improvements most affected, especially in relation to composite laminated plates' geometries, such as a stiffener or a hole considered structural weaknesses and loading conditions. Instead of focusing on the plate's external dimensions, the researchers propose that damping and stiffness may be increased by reversing the direction of fibers in the layers and altering the distribution of fibers in response to load conditions [9] to their conviction that the lamination sequence on response can be used to more accurately describe the reaction at all points in a fibre-reinforced structure and examine stresses, strains, and failure [10]. Understanding the kind of failure that occurs most of the time helps the route of improvement selection be more efficient and less costly by taking into account the compatibility of these improvements with the quality of the structure and the specificity of the position of the plates in it. For example, edge stiffeners may enhance plate stiffness, which may conflict with the structure's shape. So, the resort to increasing the thickness or changing the direction of the fibers to reduce the effect of the axial load applied in the same order of the distribution fibre is more convenient [11].

For this reason, the findings of Kuo & Shiau (2009) element analysis of composite laminated plates with variable fibre spacing, are very noteworthy. Like their predecessors, this showed that every gain in the qualities of composite materials might lead to their weakness in other areas. The critical buckling load may be increased, for example, by the fibers scattered throughout the plate's perimeter. However, adding bulk rather than stiffness will reduce the natural frequencies. The stiffness and mass of a plate may be altered by altering the distribution of fibers. As a result, the natural mode's sequence may be adjusted [12]. This study provides a cross -ply composite laminated plate and optimizes by modifying the fibre distribution and aggregation in just one particular region of the material and establishing a degree of plate layer variability in that specific location. A further advantage of this research is that it will resist buckling and shearing under in-plane compression loads since the direction of the transverse stress is not always the same as the fibre direction. As a point of reference for any study into enhancing the qualities of composite panels with variable fibre distribution, Leissa & Martin (1990) [13] advocated this improvement in fibre orientations.

2. Literature Review

Al-Mosawi [14] studied the effect of variable fibre spacing on post-buckling of boron/epoxy fibre-reinforced laminated composite plate, which examined the impact of fibre distribution on a sample subjected to a static load in plan loading, as well as other influencing factors with each distribution equation through non-linear static analysis under in-plane forces like direction compression load and various fibre orientations [1]. The study was not sufficient to understand the effect of the difference in the distribution of fibers in the composite panels with the rotation of those fibers, as well as the election of the static load in the study did not give the critical state of the buckling stresses.

Joshi & Pal (2020) [15] underlined the importance of fibre orientation and stacking sequence in terms of laminate strength and failure development. According to several theories (Ren et al. [16], Bui & Hu [17], Azzi & Tsai [18], Hoffman & Gibeling [19], Tsai [20], Hasin & Rotem [21], Rotem & Hashin [22]), the maximum stresses in anti-symmetric plates and cross ply-by-ply plates under uniform sinusoidal transverse dynamic loading were also provided with additional consequences (size mash and fibre angel orientation).

Al-Ramahee & Abodi [2] studied the effect of variable fibre spacing on the dynamic behaviour of a laminated composite plate. Non-linear dynamic analysis of laminated composite plates under in-plane load was distinguished from previous studies by the effect of the percentage of fibre volume with different fibre space based on equations by Leissa & Martin (1990) [13] on non-linear dynamic analysis of laminated composite plates under in-plane load [23].

Kumar et al. [24] analyzed the non-linear deflection and stress analysis of a laminated composite sandwich plate with an elliptical cut out under different transverse loadings in the hygro-thermal environment. For the non-linear static investigation of a laminated composite sandwich plate with an elliptical cut out, this work proposes to employ virtual displacement to represent the governing equation. Fibre orientation, load parameters, volume fractions of the fibers, plate span to thickness ratios and aspect ratios, the thickness of core and face, the position of the core, boundary conditions, environmental conditions, and transverse loading types are examined without an elliptical cut out under different transverse loads.

3. Relationships for Displacement Theory

Several Cartesian components in the mid-surface nodal displacements define the displacement at any point in the plate element. This investigation included a study of three displacement equations.

- (FSDT) First-order shear deformation theory.
- (HSDT) Higher-order shear deformation theory, with seven degrees of freedom per node.
- (HSDT) Higher-order shear deformation theory, with nine degrees of freedom per node.

Reissner-Mindlin's theory of shells, or FSDT, was used in this work, sometimes referred to as the Reissner-Mindlin theory. Timoshenko beam theory's four essential assumptions, which include transverse shear deformation and the assumption that it is constant over the thickness of the plate, are reflected in the FSDT. Thus, a shear correction factor is used [25, 26]. The assumptions of the FSDT [9] are as follows:

- Z is a linear function of the in-plane displacements (plane cross-sections that stay plane after deflection);
- Because the plate thickness is small, the displacements $[u(x,y,z), v(x,y,z)$ and $w(x,y,z)]$ are negligible in comparison;
- The strains in-plane (ε_x , ε_y and γ_{xy}) are small compared to unity;
- The transverse normal stress σ_z is insignificant;
- The transverse shear stresses (τ_{xz} and τ_{yz}) are considered constant through the plate thickness.

For this theory, the displacement representation with five degrees of freedom per node is as follows:

$$\begin{aligned} u(x, y, z, t) &= u_o(x, y, t) + z\theta_x(x, y, t) \\ v(x, y, z, t) &= v_o(x, y, t) + z\theta_y(x, y, t) \\ w(x, y, z, t) &= w_o(x, y, t) \end{aligned} \quad (1)$$

when (t) denotes the time, and $(u_o, v_o$ and $w_o)$ are the components of the mid-plane displacements for a generic point (x, y, z) having displacements $(u, v,$ and $w)$ in $(x, y,$ and $z)$ directions, respectively. Here, θ_x and θ_y are rotations of transverse normal in the (xz) and (yz) planes, respectively. The strain-displacement relations after differentiating Equation 1 are:

$$\begin{aligned} \varepsilon_x &= \frac{\partial u}{\partial x} = \varepsilon_x^o + z\kappa_x \\ \varepsilon_y &= \frac{\partial v}{\partial y} = \varepsilon_y^o + z\kappa_y \\ \gamma_{xy} &= \frac{\partial u}{\partial y} + \frac{\partial v}{\partial x} = \gamma_{xy}^o + z\kappa_{xy} \\ \gamma_{xz} &= \frac{\partial u}{\partial z} + \frac{\partial w}{\partial x} = \phi_x \\ \gamma_{yz} &= \frac{\partial v}{\partial z} + \frac{\partial w}{\partial y} = \phi_y \end{aligned} \quad (2)$$

where;

$$\begin{aligned} \varepsilon_x^o &= \frac{\partial u_o}{\partial x}, \quad \varepsilon_y^o = \frac{\partial v_o}{\partial y}, \quad \gamma_{xy}^o = \frac{\partial u_o}{\partial y} + \frac{\partial v_o}{\partial x} \\ \kappa_x &= \frac{\partial \theta_x}{\partial x}, \quad \kappa_y = \frac{\partial \theta_y}{\partial y}, \quad \kappa_{xy} = \frac{\partial \theta_x}{\partial y} + \frac{\partial \theta_y}{\partial x} \\ \phi_x &= \theta_x + \frac{\partial w_o}{\partial x} \\ \phi_y &= \theta_y + \frac{\partial w_o}{\partial y} \end{aligned} \quad (3)$$

There is a centre plane in the laminate where all of these stresses are determined. For any lamina orientation, substituting Equation 2 into the equation of the stress-strain connections results in:

$$\begin{bmatrix} \sigma_x \\ \sigma_y \\ \tau_{xy} \\ \tau_{xz} \\ \tau_{yz} \end{bmatrix} = \begin{bmatrix} Q_{11} & Q_{12} & Q_{16} & 0 & 0 \\ Q_{12} & Q_{22} & Q_{26} & 0 & 0 \\ Q_{16} & Q_{26} & Q_{66} & 0 & 0 \\ 0 & 0 & 0 & Q_{55} & Q_{45} \\ 0 & 0 & 0 & Q_{45} & Q_{44} \end{bmatrix} \begin{bmatrix} \varepsilon_x \\ \varepsilon_y \\ \gamma_{xy} \\ \gamma_{xz} \\ \gamma_{yz} \end{bmatrix} \quad (4)$$

The stress-strain relations for L^{th} lamina are as follows:

$$\begin{bmatrix} \sigma_x \\ \sigma_y \\ \tau_{xy} \end{bmatrix}^L = \begin{bmatrix} Q_{11} & Q_{12} & Q_{16} \\ Q_{12} & Q_{22} & Q_{26} \\ Q_{16} & Q_{26} & Q_{66} \end{bmatrix} \left\{ \begin{bmatrix} \varepsilon_x^o \\ \varepsilon_y^o \\ \gamma_{xy}^o \end{bmatrix} + z \begin{bmatrix} \kappa_x \\ \kappa_y \\ \kappa_{xy} \end{bmatrix} \right\} \quad (5)$$

$$\begin{bmatrix} \tau_{xz} \\ \tau_{yz} \end{bmatrix}^L = \begin{bmatrix} Q_{55} & Q_{45} \\ Q_{45} & Q_{44} \end{bmatrix} \begin{bmatrix} \phi_x \\ \phi_y \end{bmatrix} \quad (6)$$

The stress, moment, and shear resultants of NL-layered laminate are:

$$\begin{bmatrix} N_x \\ N_y \\ N_{xy} \end{bmatrix}^L = \int_{-h/2}^{h/2} \begin{bmatrix} \sigma_x \\ \sigma_y \\ \tau_{xy} \end{bmatrix} dz = \sum_{L=1}^{NL} \begin{bmatrix} Q_{11} & Q_{12} & Q_{16} \\ Q_{12} & Q_{22} & Q_{26} \\ Q_{16} & Q_{26} & Q_{66} \end{bmatrix}^L \left(\int_{h_{L-1}}^{h_L} \left\{ \begin{bmatrix} \varepsilon_x^o \\ \varepsilon_y^o \\ \gamma_{xy}^o \end{bmatrix} + z \begin{bmatrix} \kappa_x \\ \kappa_y \\ \kappa_{xy} \end{bmatrix} \right\} dz \right) \quad (7)$$

$$\begin{bmatrix} M_x \\ M_y \\ M_{xy} \end{bmatrix}^L = \int_{-h/2}^{h/2} \begin{bmatrix} \sigma_x \\ \sigma_y \\ \tau_{xy} \end{bmatrix} z dz = \sum_{L=1}^{NL} \begin{bmatrix} Q_{11} & Q_{12} & Q_{16} \\ Q_{12} & Q_{22} & Q_{26} \\ Q_{16} & Q_{26} & Q_{66} \end{bmatrix}^L \left(\int_{h_{L-1}}^{h_L} \left\{ z \begin{bmatrix} \varepsilon_x^o \\ \varepsilon_y^o \\ \gamma_{xy}^o \end{bmatrix} + z^2 \begin{bmatrix} \kappa_x \\ \kappa_y \\ \kappa_{xy} \end{bmatrix} \right\} dz \right) \quad (8)$$

$$\begin{bmatrix} Q_x \\ Q_y \end{bmatrix}^L = \int_{-h/2}^{h/2} \begin{bmatrix} \tau_{xz} \\ \tau_{yz} \end{bmatrix} dz = \sum_{L=1}^{NL} \begin{bmatrix} Q_{55} & Q_{45} \\ Q_{45} & Q_{44} \end{bmatrix}^L \left(\int_{h_{L-1}}^{h_L} \left\{ \begin{bmatrix} \phi_x \\ \phi_y \end{bmatrix} \right\} dz \right) \quad (9)$$

The stress-resultant/strain relationships of the laminate are defined as follows in a matrix form after integration

$$\begin{bmatrix} N_x \\ N_y \\ N_{xy} \\ M_x \\ M_y \\ M_{xy} \end{bmatrix} = \begin{bmatrix} A_{11} & A_{12} & A_{16} & B_{11} & B_{12} & B_{16} \\ A_{12} & A_{22} & A_{26} & B_{12} & B_{22} & B_{26} \\ A_{16} & A_{26} & A_{66} & B_{16} & B_{26} & B_{66} \\ B_{11} & B_{12} & B_{16} & D_{11} & D_{12} & D_{16} \\ B_{12} & B_{22} & B_{26} & D_{12} & D_{22} & D_{26} \\ B_{16} & B_{26} & B_{66} & D_{16} & D_{26} & D_{66} \end{bmatrix} \begin{bmatrix} \varepsilon_x \\ \varepsilon_y \\ \gamma_{xy} \\ \kappa_x \\ \kappa_y \\ \kappa_{xy} \end{bmatrix} \quad (10)$$

$$\begin{bmatrix} Q_x \\ Q_y \end{bmatrix} = \begin{bmatrix} A_{55} & A_{45} \\ A_{45} & A_{44} \end{bmatrix} \begin{bmatrix} \phi_x \\ \phi_y \end{bmatrix} \quad (11)$$

All the coefficients in A, B, and D will be defined later. Equations 10 and 11 represent the relation between the stress resultant (membrane forces, bending moments and shear forces) and the strains.

4. Materials and Methods

In previous studies on the non-linear dynamic analysis of a square plate with fibre distribution, an aspect ratio of 1 was employed, as was the slenderness ratio of 100 (Figure 1). The FENSDAAP computer program is coded in FORTRAN 94 language, the structure chart of this program is shown in Figure 2, based on the previous finite element model has been upgraded to solve twenty-five numerical samples on the large displacement analysis of composite plate. The results of the software are used to verify the reliability of the results by conforming to Al-Ramahee et al. [2] to achieve verification of the effectiveness and quality of the improvements and their suitability to avoid side effects raised by the first improvement. The isoperimetric nine-node Lagrangian elements have five degrees of freedom per node (w , θ_x , θ_y , θ_x^* , θ_y^*) and are split into a 2×2 element mesh (Table 1). Figure 3 shows the analysis results using a time step (Δt) of 0.0001 sec. Based on the new task, four previously investigated distribution patterns were selected for reanalysis, each with changes in the fiber volume fraction (V_f), as shown in Table 2. There are two types of fiber distributions here, with maximum values of 100% and 75%. As can be seen in Table 2, the average value of V_f for each distribution is provided (V_{fav}). The boron fibers and epoxy matrix utilized in the assessment are all needed for the experiment. $E_f = 413.68$ GPa, $E_m = 4.3$ GPa, $G_f = 172.36$ GPa, $G_m = 1.277$ GPa, $\nu_f = 0.2$, and $\nu_m = 0.35$ are the material's characteristics [7].

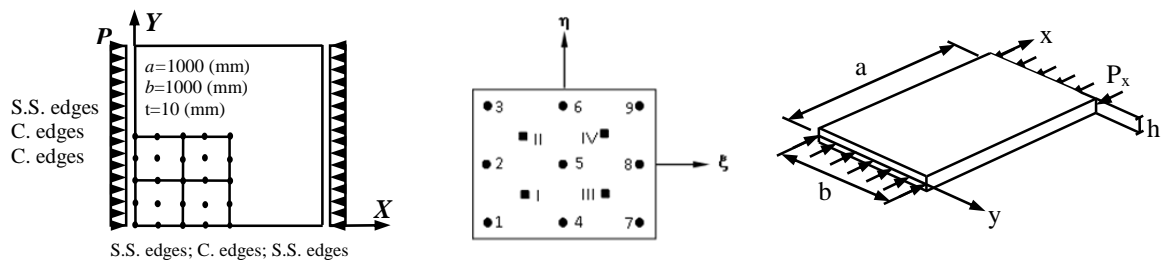


Figure 1. Description of the boundary conditions, nodes position and load direction [26]

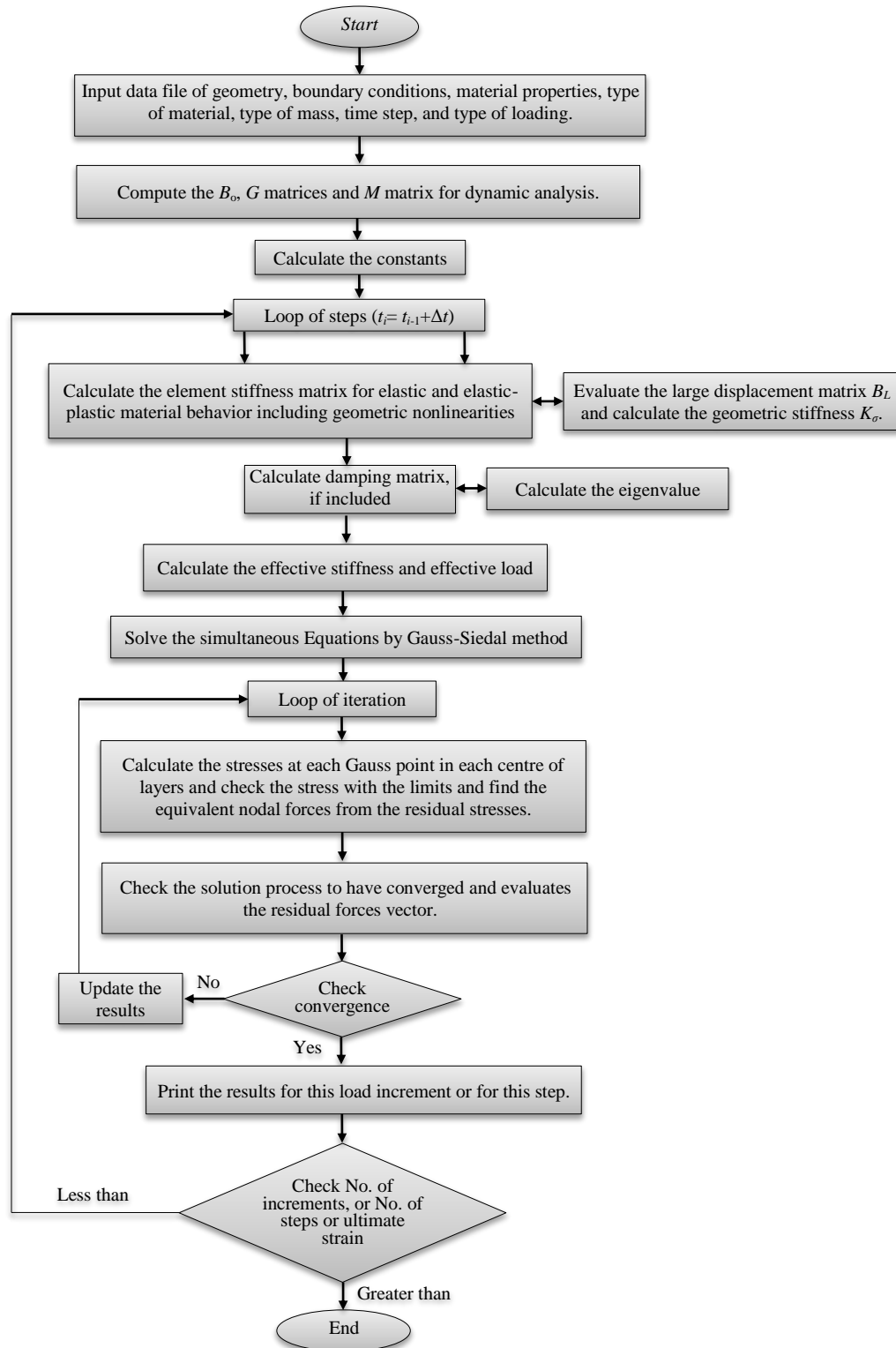


Figure 2. Structure chart of computer program (FENSDAAP) for dynamic analysis

Table 1. Showing the analyzed cases

	Case I	Case II	Case III	Case IV
Load type	Unified direction	Symmetrical	Unsymmetrical	Ply-by-ply
	$\theta (0,0,0,0)$	$\theta (0,90,90,0)$	$\theta (90,0,90,0)$	$\theta (0,30,60,90)$
Constant Rectangular Triangle Sinusoidal	Equation 1-1	Equation 1-1	Equation 1-1	Equation 1-1
	Equation 2-2	Equation 2-2	Equation 2-2	Equation 2-2
	Equation 3-3	Equation 3-3	Equation 3-3	Equation 3-3
	Equation 4-1	Equation 4-1	Equation 4-1	Equation 4-1
	Equation 5-2	Equation 5-2	Equation 5-2	Equation 5-2

Table 2. Equations of fibres distribution based on Leissa and Martine's equations [9]

Equation ($n - p$). n :equation's number p : equation's exponent	$V_f(x)$	Volume fraction of fiber (%)	
		$V_{f \max}$	$V_{f \text{av}}$
Equation 1-1	$[\frac{4}{L}X - \frac{4}{L^2}X^2]$	100	66.67
Equation 2-2	$[\frac{4}{L}X - \frac{4}{L^2}X^2]^2$	100	53.34
Equation 3-3	$[\frac{4}{L}X - \frac{4}{L^2}X^2]^3$	100	45.7
Equation 4-1	$\frac{1}{2} + [\frac{1}{L}X - \frac{1}{L^2}X^2]$	75	66.67
Equation 5-2	$\frac{1}{2} + [\frac{1}{L}X - \frac{1}{L^2}X^2]^2$	75	63.34

5. Results and Discussion

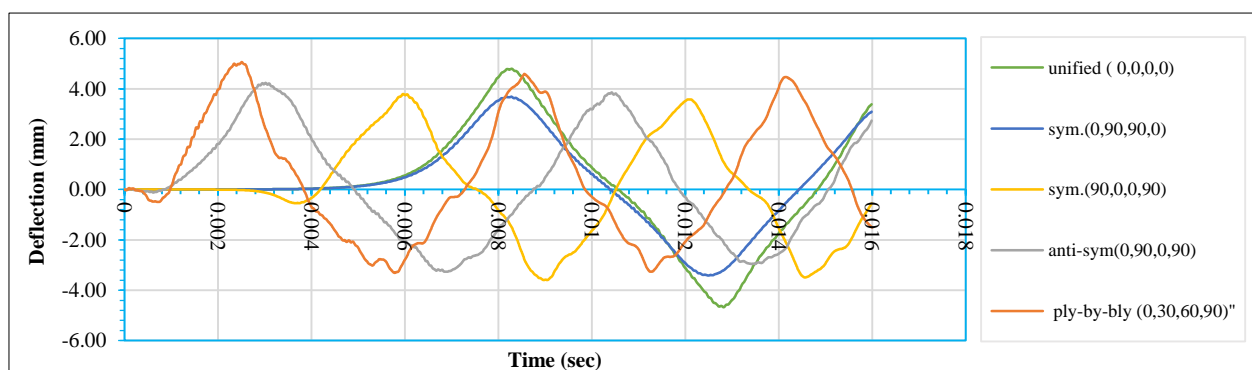
The significant variance in the excitement of the samples results from the conflict of dynamic stability among them. Dynamic stability can be defined as the sample's response to the vibration resulting from the dynamic axial load during a unit of time. It depends on the ability of the sample to dissipate the energy transmitted through it, and resulting from that load, the sample attempt to return to its original state after each case of deformation or vibration. As a result of the sample's lengthy reaction duration relative to the rest, the following indications are provided:

The significant variance in the excitement of the samples results from the conflict of dynamic stability among them. Dynamic stability can be defined as the sample's response to the vibration resulting from the dynamic axial load during a unit of time. It depends on the ability of the sample to dissipate the energy transmitted through it, and resulting from that load, the sample attempt to return to its original state after each case of deformation or vibration. As a result of the sample's lengthy reaction duration relative to the rest, the following indications are provided:

- It takes a longer time to return to its former condition than other items. A failure to rapidly disperse energy that passes through the sample might damage its internal structure and lead to an initial defect after the effective load has been removed, lowering the sample's efficiencies.
- The sample's strong displacement oscillations show stiffness within its elastic limits. As a result, it is making an effort to restore displacement to more elastic levels as rapidly as possible. Examples of this kind of simple vibrations are those produced by a sample or even a structure when it is subjected to dynamic loads or seismic vibrations within the minimum limits of vibration ineffectiveness and non-influence on the internal structure of the elements or facilities. However, oscillation within the displacement's upper limits indicates failure.

The sample's excitement compliance depends mainly on load pattern, loadings time period and manufacturing characteristics of the sample (stiffness, viscous damping, fibre distribution pattern and fibre orientation pattern). Taking into account matching other criteria and parameters such as the degree of freedom, boundary conditions, geometric properties, mass matrix type, integration method and the characteristic loads (static or dynamic, in or out- plane, and amount). This study has been analysing the influence of some parameters on dynamic stability and large elastic-plastic displacement to identify the optimum samples from which the deformation and the most stable for each loading can be identified. This study has been analysing the influence of some parameters on dynamic stability and large elastic-plastic displacement to determine the optimum samples from where the deformation and the most stable can be identified.

The first path to study the influential parameters in the behavior, large displacement and dynamic stability of orientated layered samples in various directions (cross symmetric, cross unit-symmetric and cross ply-by-ply) with a fibers uniformly distributed and homogenous within the mass matrix started by clarifying the effect of the loadings pattern in the same time period (0.0001 sec), value (500 KN/m), and direction (X-axis) in the Nonlinear dynamic analysis of this samples as shown in as detailed in Figure 2.



a) Constant load 500 (KN/m), $\Delta t = 0.0001$ (sec)

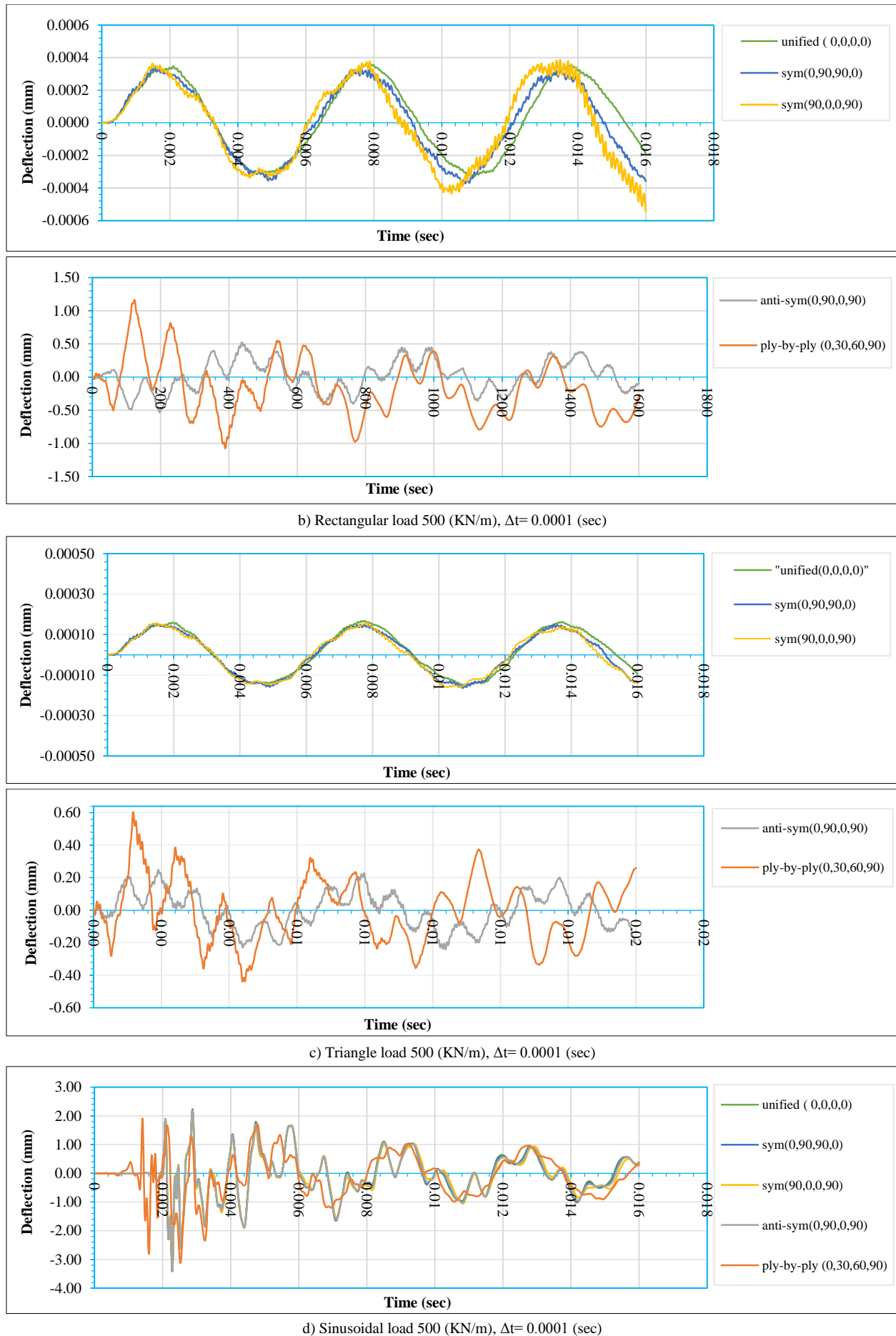


Figure 1. Non –linear dynamic analysis of large elastic-plastic displacement of the variable orientation laminated composite plates with the unified fibres distribution under different axial loads 500 (MPa), $\Delta t = 0.0001$ (sec) with X- direction

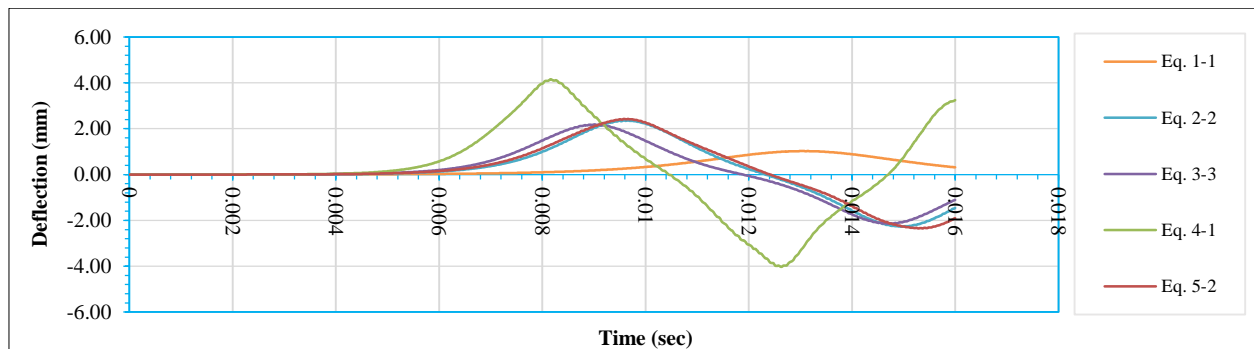
In the Figure 3:

a) Constant load: Unified direction and symmetric (0, 90, 90, 0) showed a long response within the upper limits of the displacement with high dynamic stability, symmetric (90, 0, 0, 90), anti-symmetric (90, 0, 90, 0) and cross ply-by-ply, showed a lower response than the previous ones, with the highest displacement limits and the lowest dynamic stability, symmetric (0, 90, 90, 0) was bests.

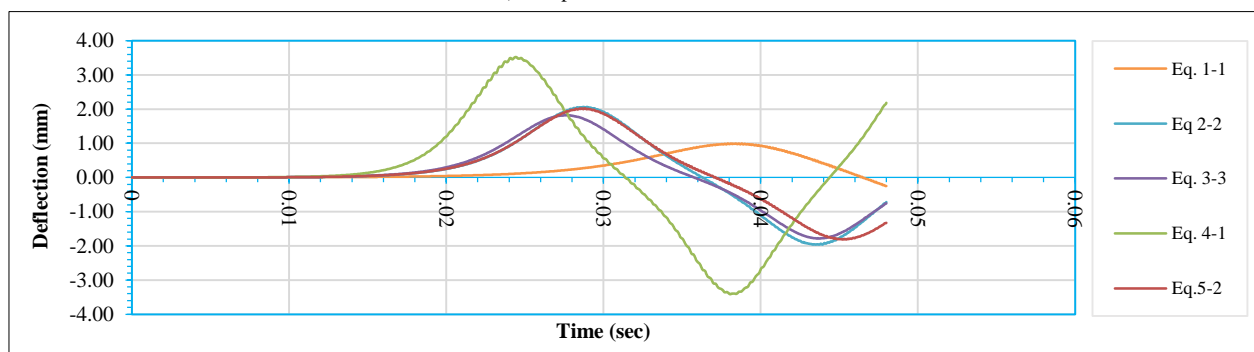
b, and c) Rectangular and Triangle load: Unified direction, symmetric (0, 90, 90, 0) and (90, 0, 0, 90) Showed a medium, regular response, and high dynamic stability, while recording very small displacements that ranged steadily between (4.0E-4 to -4.0E-4 mm), (2.0E-4 to -2.0E-4 mm) respectively. Anti-symmetric (90, 0, 90, 0) and cross ply-by-ply, It C showed high oscillation in displacement values with clarified dynamic instability and much larger displacements than predecessors in a and d.

d) Sinusoidal load: Unified direction, symmetric (0, 90, 90, 0) and (90, 0, 0, 90) showed the lowest response and highest dynamic stability, and rapid accretion of displacement after a late response, reaching the upper limits. Anti-symmetric (90, 0, 90, 0) and cross ply-by-ply, showed low response with accretion increase in displacement and good dynamic stability.

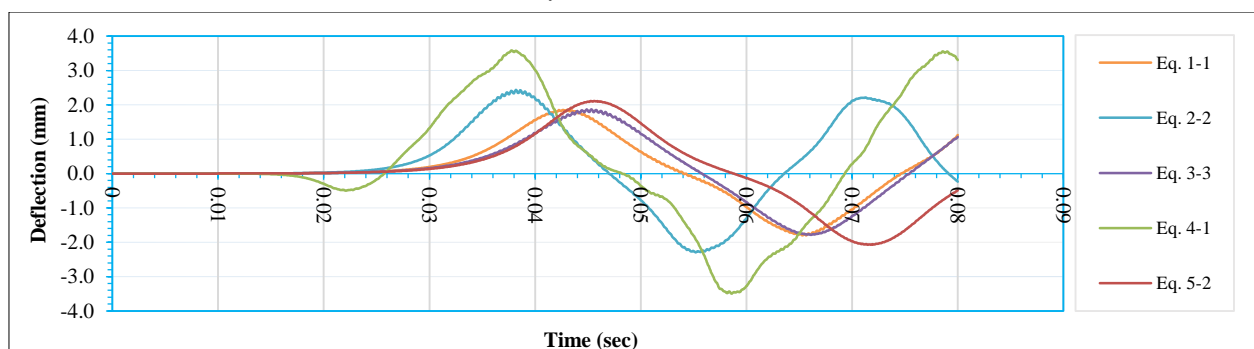
After checking the effect of loading pattern on the displacement and dynamic stability and dynamical response and distinguish the difference between the results of the different rotation patterns with the unified fibre distribution. The non-linear dynamic analysis for a several samples with different fibres distribution patterns (Eq. 1-1, Eq. 2-2, Eq. 3-3, Eq. 4-1 and Eq. 5-2) and with different layers rotation patterns (unified, symmetric (90, 0, 0, 90), symmetric (0, 90, 90, 0), anti-symmetric (90, 0, 90, 0) and cross ply-by-ply (0, 30, 60, 90) under a several axial loads (constant, rectangular, triangle, harmonic) was the second path of study as showed in Figure 4.



a) Comparison results of Case I

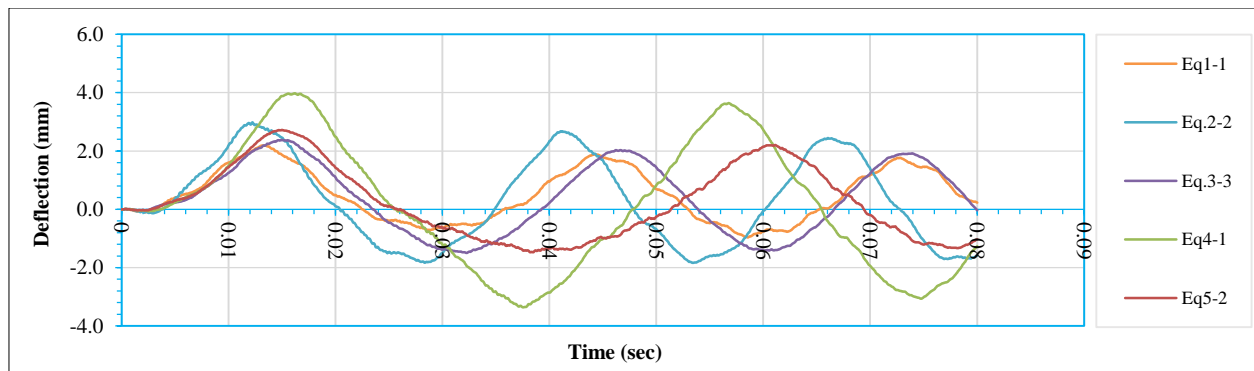


b1) [symmetrical (0, 90, 90, 0)]

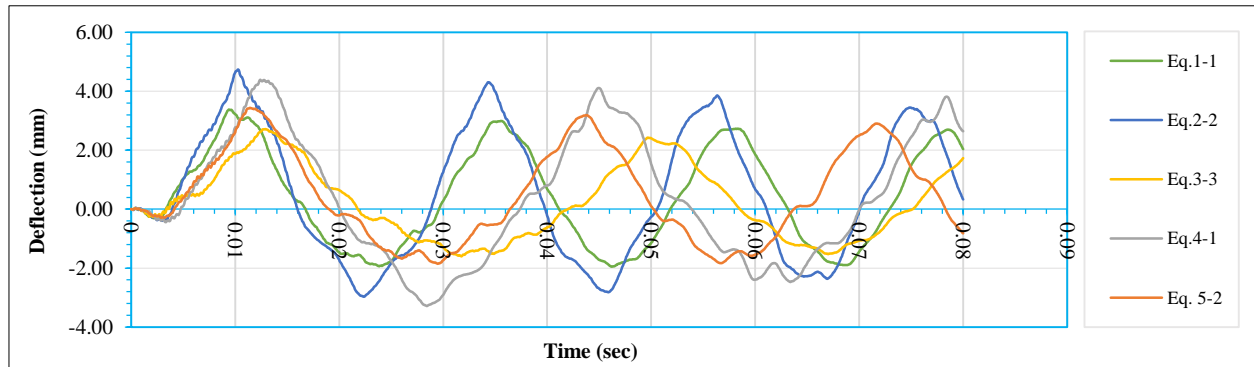


b2) [symmetrical (90, 0, 0, 90)]

b) Comparison Results for Case II



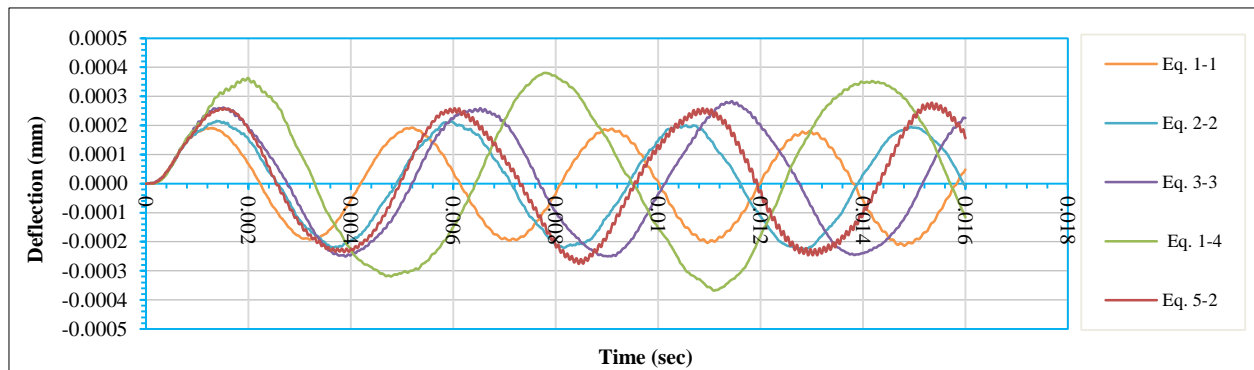
c) Comparison results for Case III



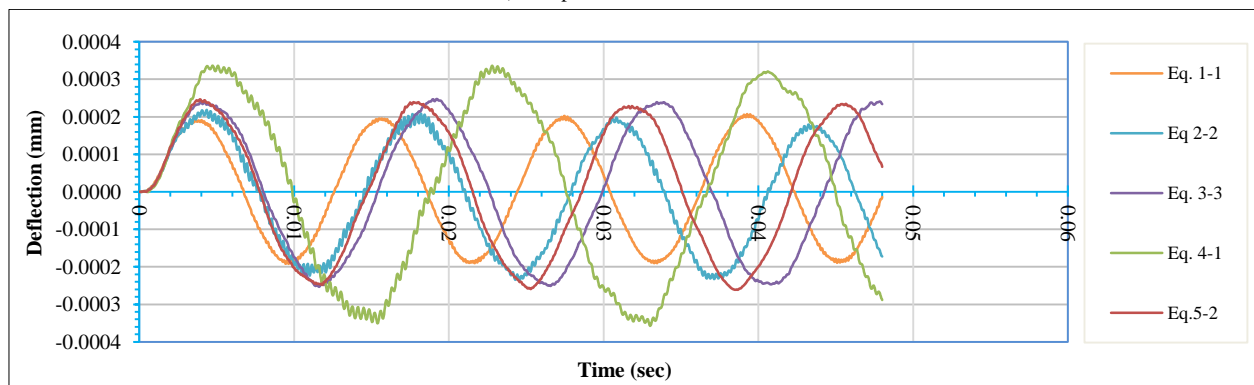
d) Comparison results for Case IV

Figure 2. Non –linear dynamic analysis of large elastic-plastic displacement of the laminated composite variable directions plates under axial constant load 500 (KN/m), $\Delta t = 0.0001$ (sec) with X- direction

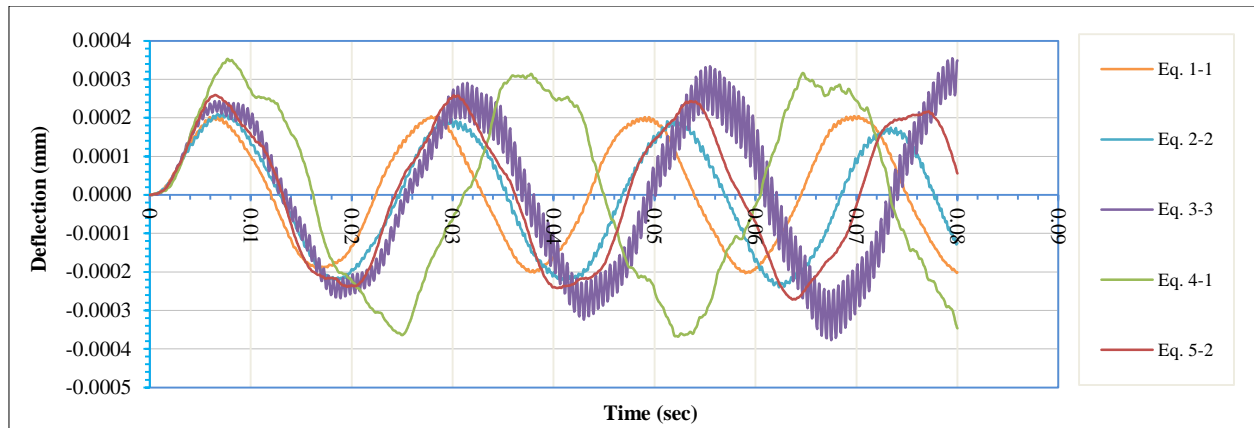
Figure 5 indicates that despite being extended beyond the top limits of the displacement (ranged 2-4 mm), the sample response variation has the direction of different layers and is an advantage of the constant load pattern. Despite the rotation having a substantial impact on the behaviour of these samples, the difference in distribution still controlled the displacement values, making Equation 1-1 distribution the best sample.



a) Comparison results of Case I

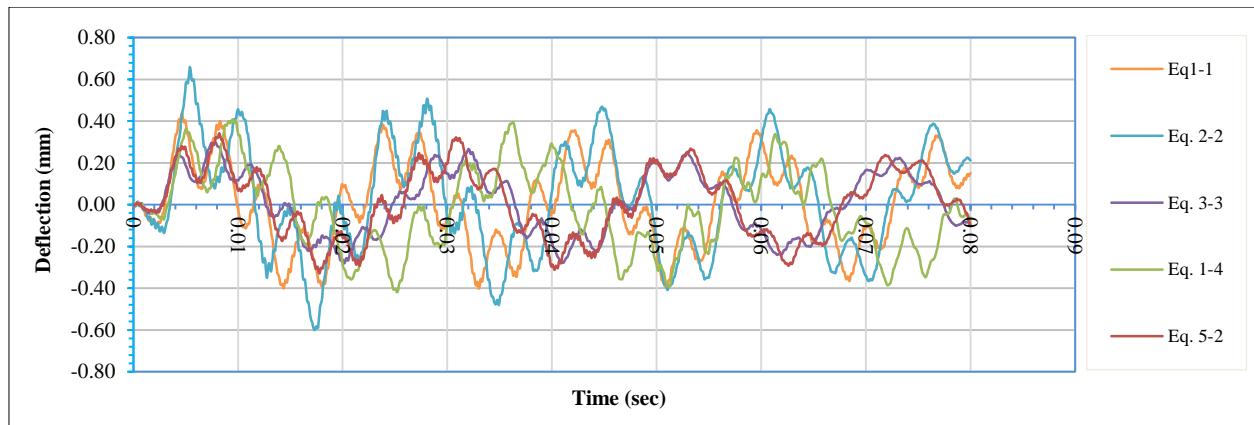


b1) [symmetrical (0, 90, 90, 0)]

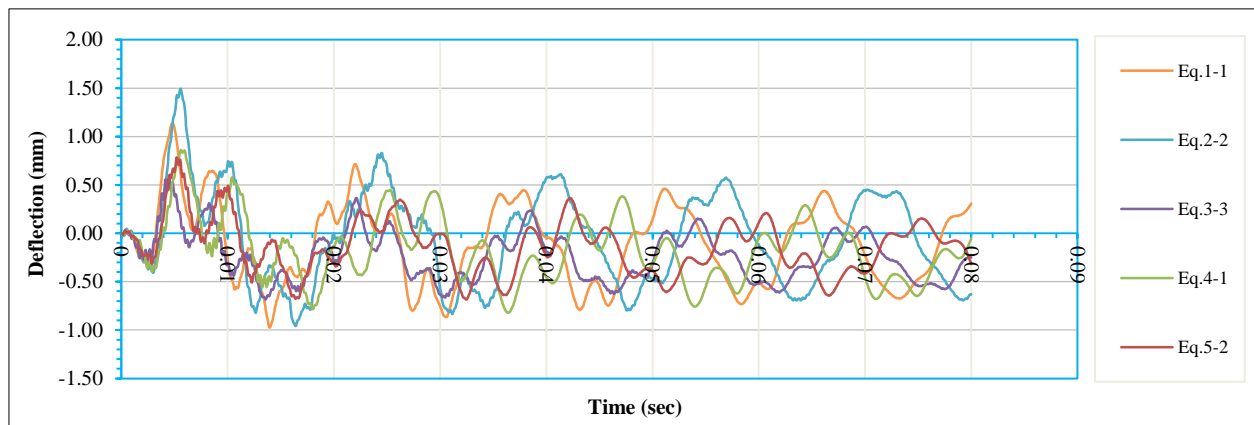


b2) [symmetrical (90, 0, 0, 90)]

b) Comparison Results for Case II



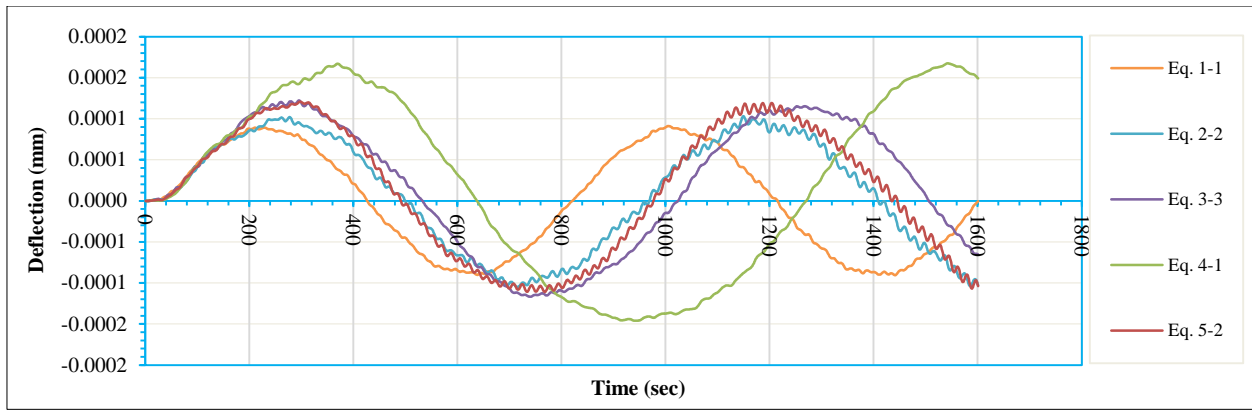
c) Comparison results for Case III



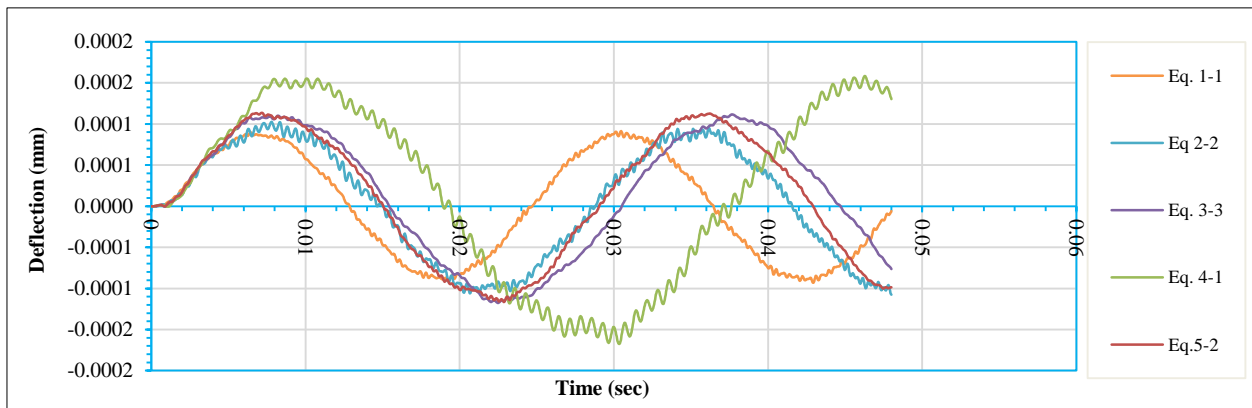
d) Comparison results for Case IV

Figure 3. Non –linear dynamic analysis of large elastic-plastic displacement of the laminated composite variable directions plates under axial rectangular load 500 (KN/m), $\Delta t = 0.0001$ (sec) with X- direction

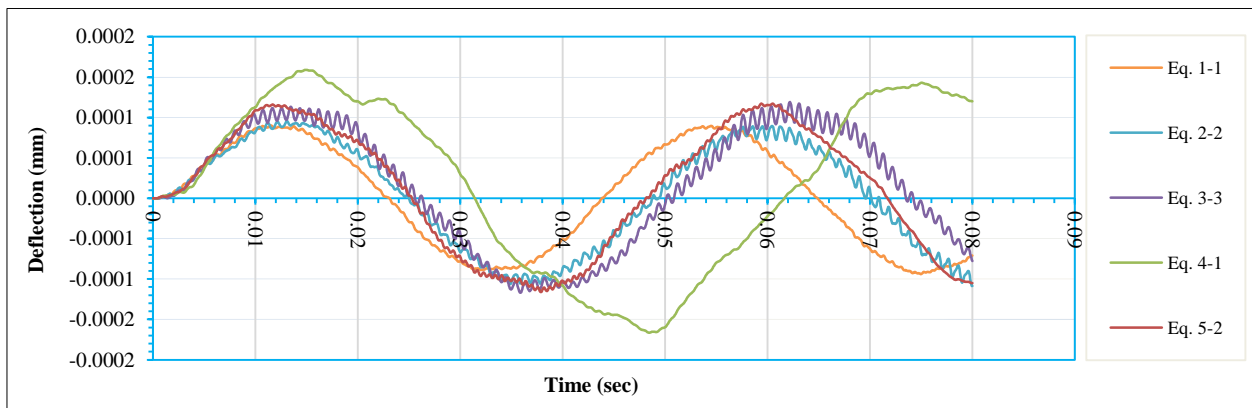
In Figure 6, the displacements in the unified direction samples and the symmetric samples were very small because of the loading pattern change ($4E-4$ to $-2E-2$ mm). It is represented by an invisible vibration that travels like a wave inside the sample, and it cannot be considered a real distortion. The anti-symmetric and cross ply-by-ply samples had higher displacements (1.5–0.5 mm) but showed a higher resistance to deformation and their attempts to return themselves to their normal position were fast and strong, so that it showed a very high oscillation within the limits of medium deformation, in same context , the sample has a fibre distribution according the Equation 3-3 with symmetric orientation showed a very large internal oscillation, as it gave more than one value for the displacement for the same time and along period time of loading, this due to generated a failure in the internal constructor of the sample, such as the separation of its layer or the occurrence of an initial malformation at the beginning of the loading that's why it's the worst.



a) Comparison results of case I

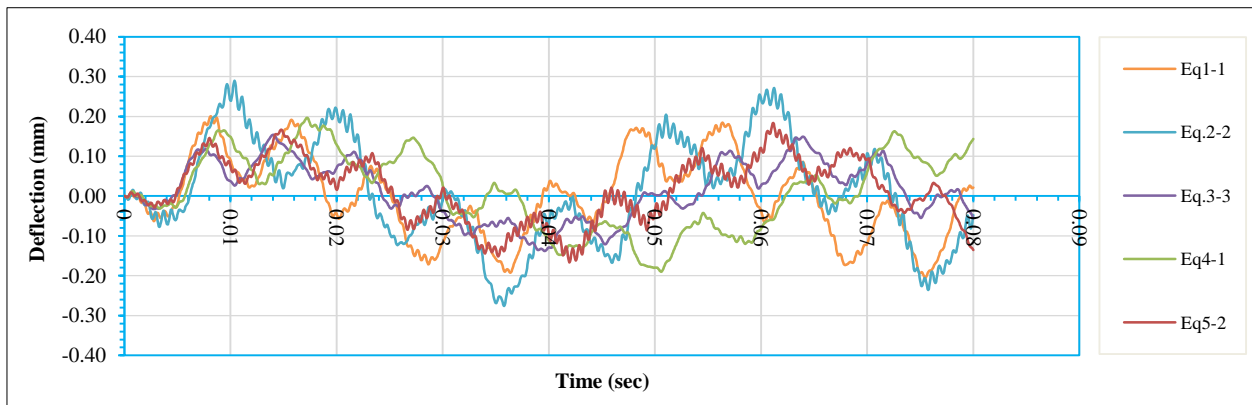


b1) [symmetrical (0, 90, 90, 0)]

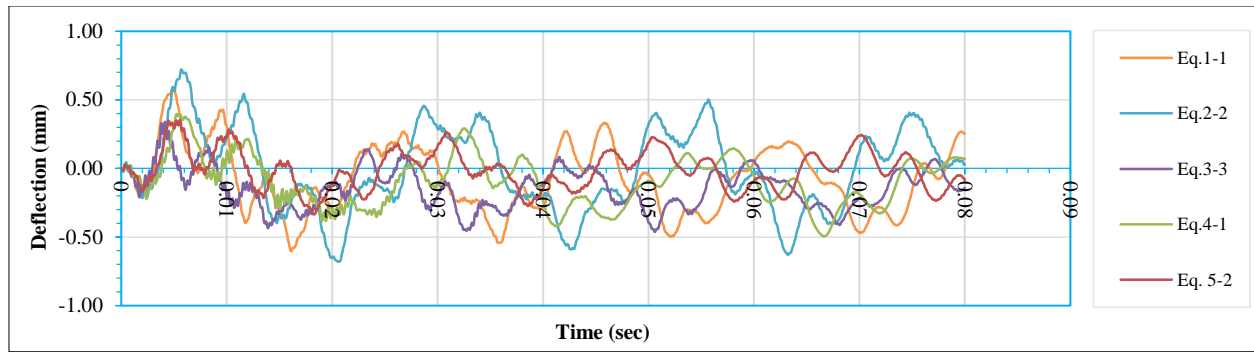


b2) [symmetrical (90, 0, 0, 90)]

b) Comparison Results for Case II



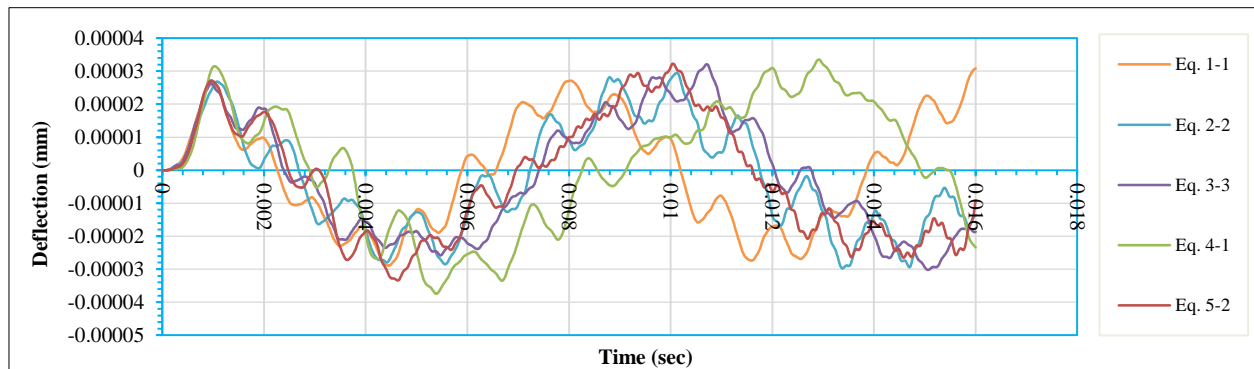
c) Comparison results for case III



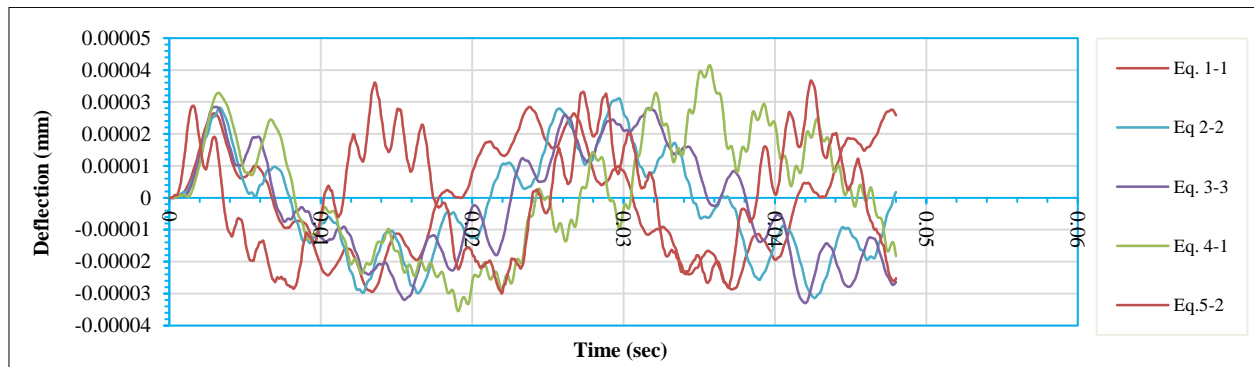
d) Comparison results for case IV

Figure 4. Non –linear dynamic analysis of large elastic-plastic displacement of the laminated composite variable directions plates under axial Triangle load 500 (KN/m), $\Delta t=0.0001$ (sec) with X- direction

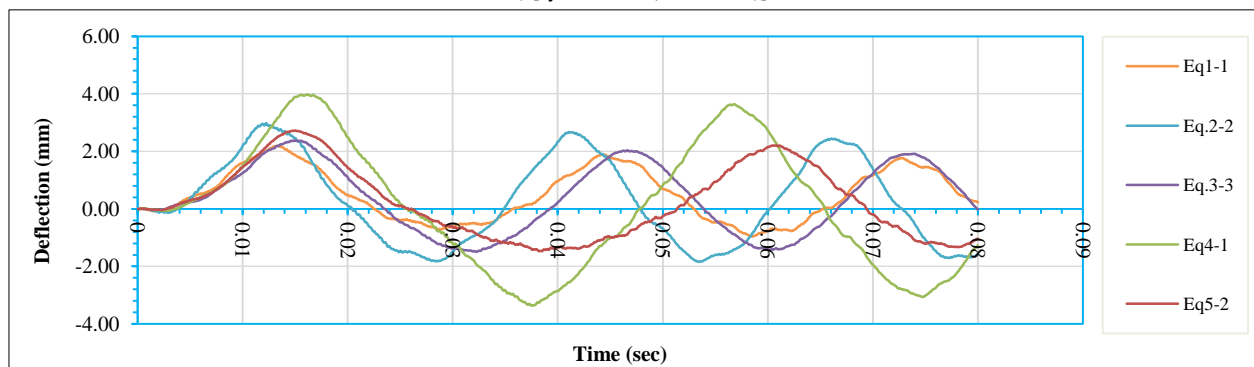
In Figure 7, the behaviour of the unified direction and cross-symmetric samples is very similar to what was detailed in the rectangular load, with lower displacement values and slightly more response and increased oscillations of the displacement curve to include Equation 2-2 in addition to Equation 3-3 in the previous loading As for the cross anti-symmetric and cross ply-by-ply samples, it showed a clear lack of response generated oscillation significantly within the lower limits of displacement with much lower displacement values than its predecessors much.



a) Comparison results of Case I

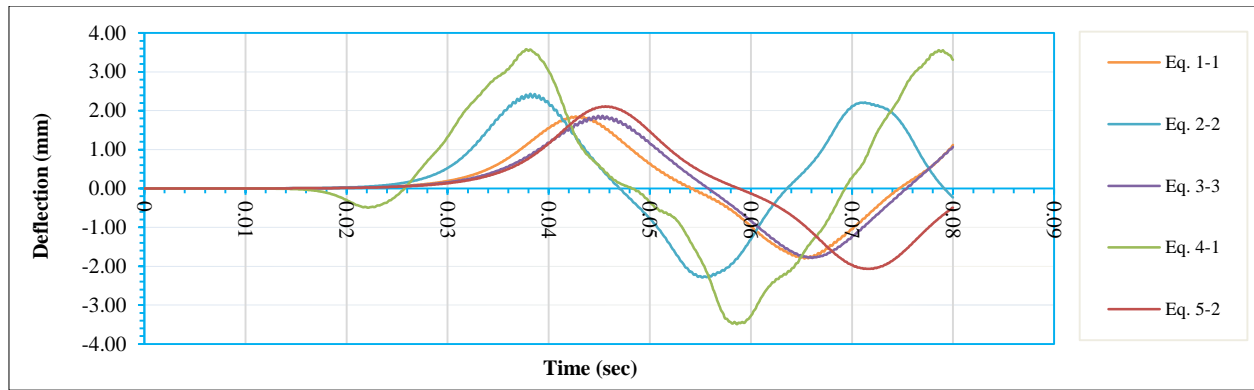


b1) [symmetrical (0, 90, 90, 0)]

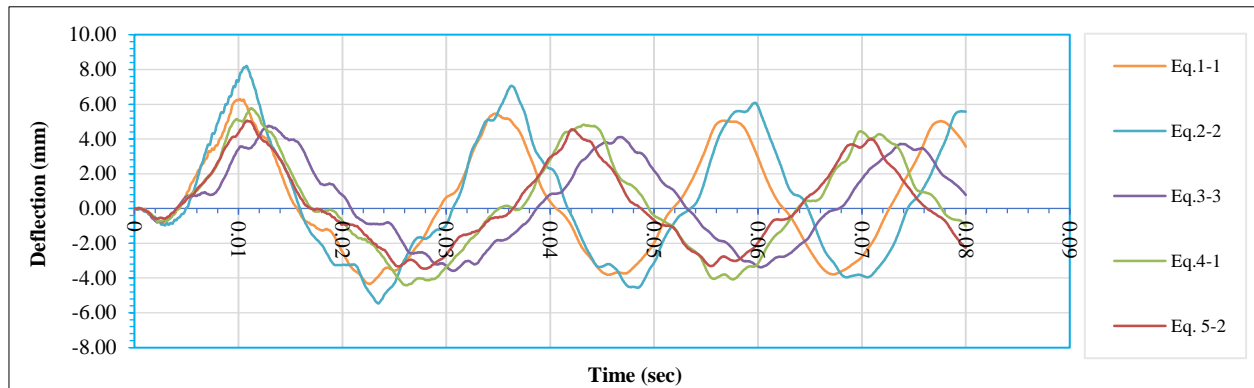


b2) [symmetrical (90, 0, 0, 90)]

b) Comparison Results for Case II



c) Comparison results for Case III



d) Comparison results for Case IV

Figure 5. Non-linear dynamic analysis of large elastic-plastic displacement of the laminated composite variable directions plates under axial sinusoidal load 500 (KN/m), $\Delta t=0.0005$ (sec) with X- direction

6. Conclusions

- Impact different patterns loading had been applied to a cross-ply laminated composite plate with unified fiber distribution, it had given a clear indication of the sensitivity of the composite panels to some loads more than others, such as constant and sinusoidal loads with all orientations, which had peak displacement elasticity, while, its effect was almost non-existent for the other rectangular and triangular loads with unified and cross-symmetrical fibers directions;
- Through programming the model, are evidenced the most influential in the results of the non-linear dynamic analysis of the laminated composite plate was the loading pattern type, magnitude, direction and its time period. Therefore, attention should be paid to studying this when discussing the use of this type of plate;
- The anti-cross symmetrical and cross ply-by-ply (0, 30, 60, 90) gave the worst results for all study cases, so we do not recommend their use;
- The distribution equations gave a clear contrast, among, which it is possible to clearly distinguish the influence of the distributions of fiber in the laminated composite plate with different orientations, which favoured Equations 1-1 and 2-2 to be the efficient distributions;
- The dynamic stability and absence of oscillation of the sample are essential factors for achieving the optimal plate after getting the least elastic displacement, able doing by increasing the damping ratio, adding elements, or creating folds to increase the stiffness.

7. Declarations

7.1. Author Contributions

Conceptualization, W.M. and H.A.; methodology, S.S.; software, W.M.; validation, W.M., S.S. and H.A.; formal analysis, W.M.; investigation, W.M.; resources, S.S.; data curation, W.M.; writing—original draft preparation, W.M.; writing-review and editing, S.S.; visualization, W.H and S.S.; supervision, S.S. and H.A.; project administration, W.M. and H.A.; funding acquisition, W.M. All authors have read and agreed to the published version of the manuscript.

7.2. Data Availability Statement

The data presented in this study are available in article.

7.3. Funding

The authors received no financial support for the research, authorship, and/or publication of this article.

7.4. Conflicts of Interest

The authors declare no conflict of interest.

8. References

- [1] Akhavan, H., Ribeiro, P., & De Moura, M. F. S. F. (2013). Large deflection and stresses in variable stiffness composite laminates with curvilinear fibres. *International Journal of Mechanical Sciences*, 73, 14–26. doi:10.1016/j.ijmecsci.2013.03.013.
- [2] Al-Ramahee, M. A., & Abodi, J. T. (2020). Effect of variable fiber spacing on dynamic behavior of a laminated composite plate. *Journal of Green Engineering*, 10(11), 12663–12677.
- [3] Zhu, C. D., & Yang, J. (2019). Free and forced vibration analysis of composite laminated plates. 26th International Congress on Sound and Vibration, 7-11 July, 2019, Montreal, Canada.
- [4] Markad, K. M., Das, V., & Lal, A. (2022). Deflection and stress analysis of piezoelectric laminated composite plate under variable polynomial transverse loading. *AIP Advances*, 12(8), 85024. doi:10.1063/5.0104568.
- [5] Martinez, J. R., & Bishay, P. L. (2021). On the stochastic first-ply failure analysis of laminated composite plates under in-plane tensile loading. *Composites Part C: Open Access*, 4(October), 100102. doi:10.1016/j.jcomc.2020.100102.
- [6] Farsadi, T., Asadi, D., & Kurtaran, H. (2021). Fundamental frequency optimization of variable stiffness composite skew plates. *Acta Mechanica*, 232(2), 555–573. doi:10.1007/s00707-020-02871-9.
- [7] Soufeiani, L., Ghadyani, G., Hong Kueh, A. B., & Nguyen, K. T. Q. (2017). The effect of laminate stacking sequence and fiber orientation on the dynamic response of FRP composite slabs. *Journal of Building Engineering*, 13, 41–52. doi:10.1016/j.jobbe.2017.07.004.
- [8] Khodzaev, D. (2019). Dynamic calculation of nonlinear oscillations of viscoelastic orthotropic plate with a concentrated mass. *E3S Web of Conferences*, 91, 02045. doi:10.1051/e3sconf/20199102045.
- [9] El Bouhmidi, A., & Rougui, M. (2018). Analysis of buckling phenomenon of rectangular laminated plates with a hole under different boundary conditions. *MATEC Web of Conferences*, 149, 02013. doi:10.1051/mateconf/201814902013.
- [10] Sharma, S. (2021). *Composite Materials: Mechanics, Manufacturing and Modeling*. CRC Press< Boca Raton, United States.
- [11] Georgantzinos, S. K., Antoniou, P. A., Giannopoulos, G. I., Fatsis, A., & Markolefas, S. I. (2021). Design of laminated composite plates with carbon nanotube inclusions against buckling: Waviness and agglomeration effects. *Nanomaterials*, 11(9), 2261. doi:10.3390/nano11092261.
- [12] Kuo, S. Y., & Shiau, L. C. (2009). Buckling and vibration of composite laminated plates with variable fiber spacing. *Composite Structures*, 90(2), 196–200. doi:10.1016/j.compstruct.2009.02.013.
- [13] Leissa, A. W., & Martin, A. F. (1990). Vibration and buckling of rectangular composite plates with variable fiber spacing. *Composite structures*, 14(4), 339–357. doi:10.1016/0263-8223(90)90014-6.
- [14] Al-Mosawi, A. I. (2013). Effect of variable fiber spacing on post-buckling of boron/epoxy fiber reinforced laminated composite plate. *Applied Mechanics and Materials*, 245, 126–131. Trans Tech Publications Ltd. doi:10.4028/www.scientific.net/AMM.245.126.
- [15] Joshi, R., Pal, P., & Duggal, S. K. (2020). Ply-by-ply failure analysis of laminates using finite element method. *European Journal of Mechanics-A/Solids*, 81, 103964. doi:10.1016/j.euromechsol.2020.103964.
- [16] Ren, B., Wu, C. T., Seleson, P., Zeng, D., Nishi, M., & Pasetto, M. (2022). An FEM-Based Peridynamic Model for Failure Analysis of Unidirectional Fiber-Reinforced Laminates. *Journal of Peridynamics and Nonlocal Modeling*, 4(1), 139–158. doi:10.1007/s42102-021-00063-0.
- [17] Bui, T. Q., & Hu, X. (2021). A review of phase-field models, fundamentals and their applications to composite laminates. *Engineering Fracture Mechanics*, 248, 107705. doi:10.1016/j.engfracmech.2021.107705.
- [18] Azzi, V. D., & Tsai, S. W. (1965). Anisotropic strength of composites. *Experimental mechanics*, 5(9), 283–288. doi:10.1007/BF02326292.
- [19] Hoffman, P. B., & Gibeling, J. C. (1995). Near-threshold fatigue crack growth in aluminum composite laminates. *Scripta Metallurgica et Materialia*, 32(6), 27989. doi:10.1016/0956-716X(95)93222-P.
- [20] Tsai, S. W. (1968). *Strength theories of filamentary structures Fundamental aspects of fiber reinforced plastic composites*. WileyInterscience, New York, United States.

- [21] Rotem, A., & Hashin, Z. (1975). Failure modes of angle ply laminates. *Journal of Composite Materials*, 9(2), 191-206. doi:10.1177/002199837500900209.
- [22] Hashin, Z., & Rotem, A. (1973). A fatigue failure criterion for fiber reinforced materials. *Journal of composite materials*, 7(4), 448-464. doi:10.1177/00219983730070040.
- [23] Martinez, J. R., & Bishay, P. L. (2021). On the stochastic first-ply failure analysis of laminated composite plates under in-plane tensile loading. *Composites Part C: Open Access*, 4, 100102. doi:10.1016/j.jcomc.2020.100102.
- [24] Kumar, R., Lal, A., & Sutaria, B. M. (2020). Non-linear deflection and stress analysis of laminated composite sandwich plate with elliptical cutout under different transverse loadings in hygro-thermal environment. *Curved and Layered Structures*, 7(1), 80-100. doi:10.1515/cls-2020-0008.
- [25] Stegmann, J., & Lund, E. (2001). *Structural Analysis of Composite Shell Structures*. Institute of Mechanical Engineering, Aalborg University, Aalborg, Denmark.
- [26] Ammash, H. K. (2008). *Nonlinear Static and Dynamic Analysis of Laminated Plates Under In-plane Forces*. Ph.D. Thesis, University of Babylon, Hillah, Iraq.